Journal of Geophysical Research: Space Physics

RESEARCH ARTICLE

10.1002/2018JA025283

Key Points:
- The catastrophe of the corona flux rope may be triggered by the decrease of its axial magnetic flux
- During the catastrophe, magnetic energy of the system contributes only a part of the energy release
- Internal energy release is found to be dominant during the catastrophe and may be the unique energy release

Correspondence to:
B. Zhuang,
zbzb@mail.ustc.edu.cn

Citation:
Zhuang, B., Hu, Y., Wang, Y., Zhang, Q., Liu, R., Gou, T., & Shen, C. (2018). Coronal flux rope catastrophe associated with internal energy release. *Journal of Geophysical Research: Space Physics*, *123*, 2513–2519. https://doi.org/10.1002/2018JA025283

Received 31 JAN 2018
Accepted 15 MAR 2018
Accepted article online 23 MAR 2018
Published online 21 APR 2018

Coronal Flux Rope Catastrophe Associated With Internal Energy Release

Bin Zhuang[1], Youqiu Hu[1], Yuming Wang[1,2], Quanhao Zhang[1], Rui Liu[1,3,4], Tingyu Gou[1], and Chenglong Shen[1,3]

[1]CAS Key Laboratory of Geospace Environment, Department of Geophysics and Planetary Sciences, University of Science and Technology of China, Hefei, China, [2]Synergetic Innovation Center of Quantum Information and Quantum Physics, University of Science and Technology of China, Hefei, China, [3]Mengcheng National Geophysical Observatory, School of Earth and Space Sciences, University of Science and Technology of China, Hefei, China, [4]Collaborative Innovation Center of Astronautical Science and Technology, Hefei, China

Abstract Magnetic energy during the catastrophe was predominantly studied by the previous catastrophe works since it is believed to be the main energy supplier for the solar eruptions. However, the contribution of other types of energies during the catastrophe cannot be neglected. This paper studies the catastrophe of the coronal flux rope system in the solar wind background, with emphasis on the transformation of different types of energies during the catastrophe. The coronal flux rope is characterized by its axial and poloidal magnetic fluxes and total mass. It is shown that a catastrophe can be triggered by not only an increase but also a decrease of the axial magnetic flux. Moreover, the internal energy of the rope is found to be released during the catastrophe so as to provide energy for the upward eruption of the flux rope. As far as the magnetic energy is concerned, it provides only part of the energy release, or even increases during the catastrophe, so the internal energy may act as the dominant or even the unique energy supplier during the catastrophe.

1. Introduction

It is generally believed that the magnetic free energy is the main energy supplier for the solar eruptions, such as flares, prominence eruptions, and coronal mass ejections (e.g., Forbes, 2000; Low, 2001). The catastrophic model of coronal magnetic flux rope is a very promising scenario to serve as a possible mechanism for triggering these eruptions (e.g., Hu & Wang, 2005; Lin et al., 2003). The catastrophe, belonging to nonlinear instability (Golubitsky, 1978; Saunders, 1980), requires a sudden transition of a flux rope system evolving from a quasi steady state into a dynamic state and is found to exist under certain conditions (e.g., Chen et al., 2006; Forbes & Isenberg, 1991; Forbes & Priest, 1995; Guo & Wu, 1998; Hu, 2001; Hu et al., 2003; Isenberg et al., 1993; Lin et al., 2001; Sun & Hu, 2005; Zhang et al., 2017). Within the catastrophe scenario, the magnetic energy which is stored in the corona is suddenly released (Chen et al., 2007; Zhang et al., 2016), and then results in a destabilization of the global magnetic field topology and an upward eruption of the flux rope.

Many numerical simulations have been carried out to study the catastrophe in different types of magnetostatic equilibrium background fields, for example, a dipolar field or a partially open dipolar field (Hu et al., 2003; Li & Hu, 2003), a quadrupolar field (Zhang et al., 2005), or other multipolar fields (Ding & Hu, 2006; Peng & Hu, 2005). It was found that a catastrophe could only take place when the magnetic energy of the system exceeds a certain threshold. Li and Hu (2003) found that the catastrophic energy threshold is about 8% larger than the corresponding fully open bipolar field energy, irrespective as to whether the background field is completely closed or partly open, or whether the magnetic energy is enhanced by an increase of annular or axial flux of the flux rope. Peng and Hu (2005) showed that the magnetic energy threshold is about 15% greater than the energy in a partly open multipolar magnetic field. Later, Sun and Hu (2005) extended the work of Hu et al. (2003) by changing the background from magnetostatic equilibrium state to a steady solar wind. They found that the magnetic energy exceeds the open field energy by about 8% if the gravity is negligible but is raised by an amount that approximately equals to the so-called excess gravitational energy associated with the flux rope mass.

Most of the previous catastrophe studies presuppose the dominant role of the magnetic energy during the catastrophe as the system magnetic field is supposed to provide extra energy for the flux rope eruption in terms of raising the kinetic and gravitational energies of the rope. This is the case for catastrophes occurring in solar active regions, where the magnetic field dominates and the magnetic energy acts as the dominant energy supplier. However, eruptions caused by catastrophes could also take place in solar quiet regions (e.g., Chen et al., 2011; Subramanian & Dere, 2001; Zhou et al., 2003), where other types of energies in addition to the magnetic energy may play subtle roles during the catastrophe. It is unknown whether the magnetic energy in this case will still be the dominant energy supplier for the catastrophe of the rope, particularly of the large-scale flux rope in the solar wind background. This paper extends the work of Sun and Hu (2005) to study the coronal flux rope catastrophe, with emphasis on the energy transformation during the catastrophe. Furthermore, we will show that a catastrophe can be triggered by not only an increase but also a decrease of the axial magnetic flux of the rope, which has never been discussed before. Section 2 gives the basic equations, numerical units, and simulation procedures. Section 3 shows the results of the flux rope catastrophe and the corresponding energy analysis. We conclude our work in Section 4.

2. Basic Equations and Solution Procedures

Following Sun and Hu (2005), we take spherical coordinates (r, θ, φ) and consider 2.5-dimensional (2.5-D) problems in the heliospheric meridional plane ($\frac{\partial}{\partial\varphi} = 0$). The 2.5-D ideal magnetohydrodynamics (MHD) equations are derived as follows:

$$\frac{\partial \rho}{\partial t} + \nabla \cdot (\rho \boldsymbol{v}) = 0, \tag{1}$$

$$\frac{\partial \boldsymbol{v}}{\partial t} + \boldsymbol{v} \cdot \nabla \boldsymbol{v} + R\nabla T + \frac{RT}{\rho}\nabla\rho + \frac{1}{\mu\rho}\left[\mathcal{L}\psi\nabla\psi + \boldsymbol{B}_\varphi \times \left(\nabla \times \boldsymbol{B}_\varphi\right)\right] + \frac{1}{\mu\rho r\sin\theta}\nabla\psi\cdot\left(\nabla\times\boldsymbol{B}_\varphi\right)\hat{\varphi} + \frac{GM_s}{r^2}\hat{\boldsymbol{r}} = 0, \tag{2}$$

$$\frac{\partial \psi}{\partial t} + \boldsymbol{v} \cdot \nabla\psi = 0, \tag{3}$$

$$\frac{\partial B_\varphi}{\partial t} + r\sin\theta\nabla\cdot\left(\frac{B_\varphi \boldsymbol{v}}{r\sin\theta}\right) + \left[\nabla\psi \times \nabla\left(\frac{v_\varphi}{r\sin\theta}\right)\right]_\varphi = 0, \tag{4}$$

$$\frac{\partial T}{\partial t} + \boldsymbol{v}\cdot\nabla T + (\gamma - 1)T\nabla\cdot\boldsymbol{v} = 0, \tag{5}$$

where ρ, $\boldsymbol{v}$, T, and ψ represent density, flow velocity, temperature, and magnetic flux function, respectively, and $\hat{r}$ and $\hat{\varphi}$ serve as the related unit vectors. The magnetic field is expressed by

$$\boldsymbol{B} = \nabla\times\left(\frac{\psi}{r\sin\theta}\hat{\varphi}\right) + \boldsymbol{B}_\varphi, \qquad \boldsymbol{B}_\varphi = B_\varphi\hat{\varphi}, \tag{6}$$

and $\mathcal{L}\psi$ appearing in equation (2) serves as

$$\mathcal{L}\psi \equiv \frac{1}{r^2\sin^2\theta}\left(\frac{\partial^2\psi}{\partial r^2} + \frac{1}{r^2}\frac{\partial^2\psi}{\partial\theta^2} - \frac{\cot\theta}{r^2}\frac{\partial\psi}{\partial\theta}\right). \tag{7}$$

R is the gas constant, μ is the blue magnetic permeability of free space, G is the gravitational constant, M_s is the mass of the Sun, and γ is the polytropic index which is set to be 1.05 in this paper. Note that taking $\gamma = 1.05$ rather than $\gamma = 5/3$ is aimed at adding an extraneous heating of the solar corona, necessary for supersonic solar wind solutions.

In the following numerical examples, the density and temperature at the base are set to be $\rho_0 = 1.67 \times 10^{-13}$ kg/m^3 and $T_0 = 2\times10^6$ K, respectively. We take ρ_0, T_0 and the solar radius $R_0 = 6.965\times10^8$ m as the basic numerical (density, temperature, and length) units, whereas other numerical units are derived as follows:

$$v_0 = \sqrt{RT_0} = 1.818\times10^5 \text{ m/s},\ t_0 = R_0/v_0 = 3.831\times10^3 \text{ s},$$
$$P_0 = \rho_0 RT_0 = 5.521\times10^{-3} \text{ Pa},\ B_0 = \sqrt{\mu_0\rho_0 v_0^2} = 8.329\times10^{-5} \text{ T},$$
$$\psi_0 = B_0R_0^2 = 4.040\times10^{13} \text{ Wb, and } W_0 = \frac{B_0^2R_0^3}{\mu_0} = 1.865\times10^{24} \text{ J}.$$

During the calculation, the magnetic strength at the equator on the solar surface is set to be 2×10^{-4} T, so its reading in numerical unit system is $B_E = 2.401$ $(2 \times 10^{-4}/8.329 \times 10^{-5})$, and the reading of the magnetic flux at the equator on the solar surface is $\psi_E = 2.401$ accordingly. The solution is further assumed to be symmetrical with respect to the equator ($\theta = \pi/2$), so that the computational domain is taken to be $1 \leq r \leq 215$, and $0 \leq \theta \leq \pi/2$, discretized into 185×92 grid points. The grid spacing along the radial direction is set to be uniform, 0.625 in between $r' = 10$ and 30 and 3 in between $r' = 140$ and 215, and increases according to a geometric series of a common ratio 1.0689 in between $r' = 1$ and 10 and 1.0207 in between $r' = 30$ and 140. A uniform mesh is adopted in the θ direction. The multistep implicit scheme developed by Hu (1989) is used to solve the MHD equations. The detailed solving procedures were described in Sun and Hu (2005) and are summarized as follows. First, giving $\psi(t, 1, \theta) = \psi_E \sin^2\theta$, construct a steady solar wind solution with a helmet streamer astride the equator. Second, let a flux rope emerge from below the streamer base and enter the streamer entirely. As to the flux rope, it is characterized by $\Phi_{\varphi c}$, Φ_{pc}, and M_c: the axial magnetic flux, the poloidal magnetic flux per unit radian, and the total mass per unit radian, respectively. Here the axial and poloidal fluxes correspond to the azimuthal and annular fluxes in Sun and Hu (2005), respectively. Third, adjust three parameters of the flux rope according to

$$\Phi_\varphi = \alpha_\varphi \Phi_{\varphi c},\ \Phi_p = \alpha_\psi \Phi_{pc},\ M = \alpha_m M_c, \tag{8}$$

where α_φ, α_ψ, and α_m are the adjustable constants. This adjustment will proceed until the catastrophe of the flux rope system takes place; that is, the catastrophic point is met. Finally, the energy analysis is achieved based on

$$W_k + W_g + W_i + W_m = W_t = \text{const}, \tag{9}$$

where W_k, W_g, and W_i are the kinetic, gravitational, and internal energies inside the flux rope; W_m is the total magnetic energy of the whole system; and the total energy W_t is the sum of these energies. Equation (9) is based on an assumption that the energy variation outside the rope is dominated by the magnetic energy. One may refer to Appendix A for details about this assumption and the energy equation. To be consistent with Sun and Hu (2005), the energy unit W_0 is changed to $4\pi B_E^2 W_0 = 1.351 \times 10^{26}$ J. As a result, the potential field with the same magnetic flux distribution at the base, that is, a dipolar field, has an energy $W_p = 1/3$, and the corresponding open field energy is $1.662 W_p = 0.554$.

3. Energy Analysis During the Catastrophe of the Flux Rope System

Following the simulations introduced above, we have constructed a steady solution with a helmet streamer and a flux rope in it. The three rope parameters are $(\Phi_\varphi,\ \Phi_p,\ M) = (\Phi_{\varphi c},\ \Phi_{pc},\ M_c) = (0.048,\ 1.000,\ 0.239)$, and the magnetic configuration is shown in Figure 1a. For simplicity, only one of these parameters is adjusted while the others remain invariant. Namely, we adjust one of the three multipliers $(\alpha_\varphi,\ \alpha_\psi,\ \alpha_m)$ in equation (8) and fix the other two to be 1 so as to find the corresponding catastrophic points. Following Sun and Hu (2005), we increase α_φ, α_ψ or decrease α_m until a catastrophic point is met, and the obtained multipliers turn out to be $(\alpha_\varphi,\ \alpha_\psi,\ \alpha_m) = (1.12,\ 1,\ 1)$, $(1,\ 1.04,\ 1)$, and $(1,\ 1,\ 0.74)$, respectively. Each catastrophic point is labeled by a set of multipliers $(\alpha_\varphi,\ \alpha_\psi,\ \alpha_m)$, as shown in Table 1. Also listed in the table are the kinetic energy W_k, the gravitational energy W_g, and the internal energy W_i of the flux rope, the magnetic energy W_m of the whole system, and the sum of these energies (W_t) right before and 10 hr after the catastrophe (see the values in the first and second rows of each catastrophic point). Besides, ΔW_i, ΔW_m, and ΔW_t represent the related energy variations during the 10 hr after catastrophe.

As the flux rope is attached to the solar surface before eruption, the kinetic energy of the rope is zero as shown in Table 1. During the catastrophe, the magnetic energy of the system and the internal energy of the flux rope are released, so the related variations and ΔW_i and ΔW_m are negative. On the other hand, the kinetic and gravitational energies of the flux rope increase, indicating an upward eruption of the flux rope. The total energy W_t is found to be approximately conserved, and the relative differences $|\Delta W_t|/\overline{W}_t$ ($\overline{W}_t$) is the averaged value of the two listed total energies at each catastrophic point) are less than 3.1%. This implies that the released magnetic energy and internal energy are responsible for the increase of the kinetic and gravitational energies. Note that the contribution made by the internal energy is comparable to and even larger than that made by the magnetic energy.

In addition to catastrophes caused by either increasing α_φ or α_ψ or decreasing α_m, as we have discussed above, we found that a catastrophe can also be triggered as α_φ decreases. The resultant catastrophic point

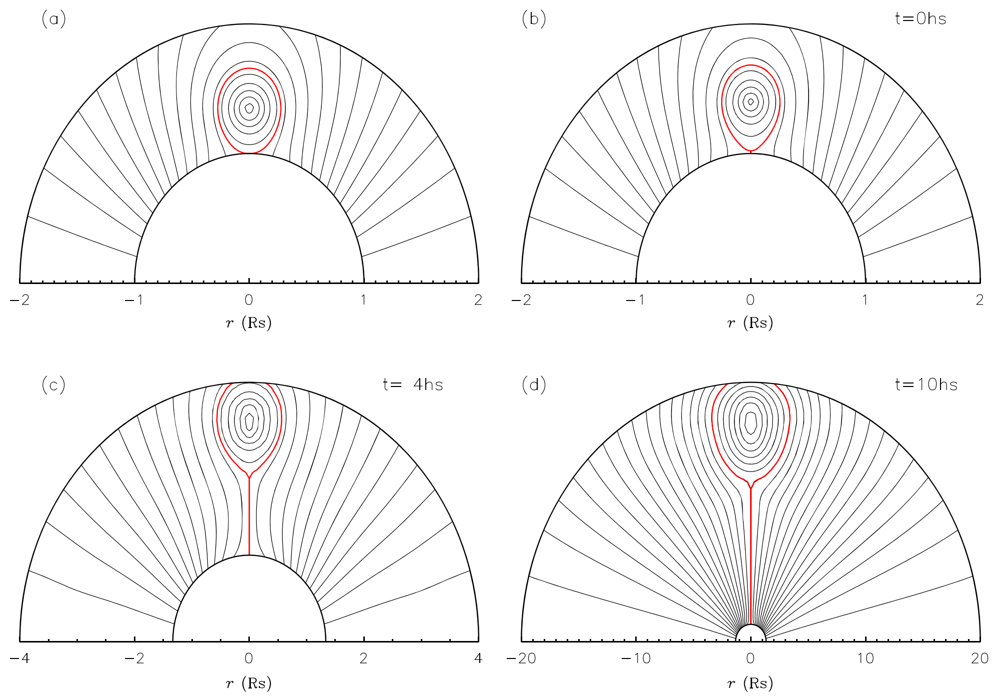

Figure 1. (a) Magnetic configuration of the flux rope system in steady state with $(\Phi_\varphi, \Phi_p, M) = (0.048, 1.000, 0.239)$. (b–d) Magnetic configurations associated with the erupting flux rope at three separate times with $(\Phi_\varphi, \Phi_p, M) = (0.026, 1.000, 0.239)$. The red closed curves indicate the border of the flux rope.

corresponds to $(\alpha_\varphi, \alpha_\psi, \alpha_m) = (0.54, 1, 1)$, leading to $(\Phi_\varphi, \Phi_p, M) = (0.026, 1.000, 0.239)$, and the related energies are listed in the last line of Table 1. Figures 1b–1d shows the magnetic configurations at three separate times associated with the eruption of the flux rope. The magnetic energy and the internal energy are both released, but the contribution made by the former is 0.0113, very small as compared with 0.1220 which is made by the latter. In order to check whether the magnetic energy can increase during a catastrophe, we tried another example in which $(\Phi_{\varphi c}, \Phi_{pc}, M_c) = (0.054, 0.9, 0.255)$. The catastrophic points, labeled by $(\alpha_\varphi, \alpha_\psi, \alpha_m)$, and the associated energies are listed in Table 2. The total energy W_t is also found to be approximately conserved, with the relative differences evaluated from the data given in Table 2 being less than 2.9%. Most results are similar to those of the previous example, except the catastrophe caused by decreasing α_φ, as listed in the last line of Table 2. The magnetic energy of the system increases instead during the catastrophe. This indicates that the magnetic field absorbs energy from the system during the catastrophe. The internal energy turns out to be the only energy supplier for the catastrophe. Besides, additional information in Tables 1

Table 1
The Energies at the Catastrophic Points Labeled by $(\alpha_\varphi, \alpha_\psi, \alpha_m)$ for $(\Phi_{\varphi c}, \Phi_{pc}, M_c)$ = (0.048, 1.000, 0.239)

$(\alpha_\varphi, \alpha_\psi, \alpha_m)$	W_k	W_g	W_i	W_m	W_t	ΔW_i	ΔW_m	ΔW_t
(1.12, 1, 1)	0.0000	−0.0881	0.3501	0.6224	0.8844	−0.0899	−0.0522	0.0125
	0.0519	−0.0104	0.2602	0.5702	0.8719			
(1, 1.04, 1)	0.0000	−0.0881	0.3445	0.6239	0.8803	−0.0986	−0.0578	0.0231
	0.0528	−0.0076	0.2459	0.5661	0.8572			
(1, 1, 0.74)	0.0000	−0.0682	0.2733	0.6146	0.8197	−0.0797	−0.0483	0.0275
	0.0392	−0.0069	0.1936	0.5663	0.7922			
(0.54, 1, 1)	0.0000	−0.0867	0.3546	0.5749	0.8428	−0.1220	−0.0113	0.0069
	0.0473	−0.0076	0.2326	0.5636	0.8359			

Note. W_k, W_g, W_i are the kinetic, gravitational, and internal energies inside the flux rope, respectively; W_m is the magnetic energy of the whole domain; and W_t is the total energy derived by the sum of these energies. ΔW_i, ΔW_m, and ΔW_t correspond to the related energy variations during the 10 hr after catastrophe.

Table 2
Same as Table 1 but Associated With ($\Phi_{\varphi c}$, Φ_{pc}, M_c) = (0.054, 0.900, 0.255)

(α_φ, α_ψ, α_m)	W_k	W_g	W_i	W_m	W_t	ΔW_i	ΔW_m	ΔW_t
(1.31, 1, 1)	0.0000	−0.0945	0.3813	0.6147	0.9015	−0.1130	−0.0497	0.0184
	0.0576	−0.0078	0.2683	0.5650	0.8831			
(1, 1.13, 1)	0.0000	−0.0943	0.3589	0.6224	0.8870	−0.0948	−0.0561	0.0078
	0.0569	−0.0081	0.2641	0.5663	0.8792			
(1, 1, 0.29)	0.0000	−0.0290	0.1147	0.5934	0.6791	−0.0301	−0.0262	0.0191
	0.0135	−0.0053	0.0846	0.5672	0.6600			
(0.26, 1, 1)	0.0000	−0.0949	0.3766	0.5313	0.8130	−0.1577	0.0266	−0.0151
	0.0556	−0.0043	0.2189	0.5579	0.8281			

and 2 is given as (1) the magnetic field of the system after the catastrophe in all examples will approach a fully open one with the corresponding W_m close to 0.554 and (2) the total energy release derived by $\Delta W_i + \Delta W_m$ approximately equals to 10^{25} J, which is comparable to the energy release of about 10^{25} to 10^{26} J during a major flare event.

4. Conclusions and Discussions

We extend the work of Sun and Hu (2005) to study the catastrophe of the coronal flux rope system in the solar wind background by a 2.5-D MHD model. In this model, a flux rope is characterized by its axial and poloidal magnetic fluxes and total mass. We analyze the kinetic, gravitational, and internal energies of the rope itself as well as the magnetic energy of the whole system. As the rope magnetic fluxes increase or the rope mass decreases, a catastrophe can be triggered, leading to an upward eruption of the flux rope. The internal energy of the rope and the magnetic energy of the system are both released, leading to an increase of the rope kinetic and gravitational energies. Furthermore, we find that a catastrophe can also be triggered as the flux rope axial magnetic flux decreases. In this case, the magnetic energy of the system provides a very small part of the energy release, or even increase during the catastrophe. The contribution of the release made by the internal energy is comparable to and even larger than that made by the magnetic energy. Furthermore, the internal energy may serve as the unique energy supplier of the flux rope catastrophe.

Note that we have taken an ideal MHD approximation, namely, magnetic reconnection is prohibited across the current sheet formed via the erupting flux rope. If magnetic reconnection is incorporated, then the magnetic field after catastrophe will approach a potential one, of which the magnetic energy is 1/3 instead of 0.554, the energy limit for a fully open field. In this case, the magnetic energy will make a much larger contribution to the catastrophe. Nevertheless, as for triggering the catastrophe, the internal energy of the flux rope plays an important role, which cannot be neglected.

Appendix A

Starting from the ideal MHD equations, one may derive the total energy equation as follows:

$$\frac{\partial w}{\partial t} + \nabla \cdot (w\boldsymbol{v}) + \nabla \cdot \left[\left(p + \frac{B^2}{2\mu_0}\right)\boldsymbol{v}\right] - \nabla \cdot \left[\frac{(\boldsymbol{v}\cdot\boldsymbol{B})\boldsymbol{B}}{\mu_0}\right] = 0. \tag{A1}$$

Here w is the energy density, expressed by

$$w = w_k + w_g + w_i + w_m, \tag{A2}$$

where

$$w_k = \frac{1}{2}\rho v^2,\ w_g = -\frac{GM_s\rho}{r},\ \ w_i = \frac{p}{\gamma - 1},\ \text{and}\ w_m = \frac{1}{2\mu_0}B^2 \tag{A3}$$

are the densities of kinetic, gravitational, internal, and magnetic energies, respectively. The total energy within the coronal flux rope is evaluated by

$$W = \iiint_{\psi \geq \psi_E} w\mathrm{d}V, \tag{A4}$$

and its time rate reads

$$\frac{\mathrm{d}W}{\mathrm{d}t} = \iiint_{\psi \geq \psi_E} \left[\frac{\partial w}{\partial t} + \nabla \cdot (w\boldsymbol{v}) \right] \mathrm{d}V, \tag{A5}$$

where the meaning of ψ_E is the magnetic flux at the flux rope border. Inserting equation (A1) into equation (A5) leads to

$$\frac{\mathrm{d}W_k}{\mathrm{d}t} + \frac{\mathrm{d}W_g}{\mathrm{d}t} + \frac{\mathrm{d}W_i}{\mathrm{d}t} + \frac{\mathrm{d}W_{m1}}{\mathrm{d}t} + \oiint_{\psi=\psi_E} \left(p + \frac{B^2}{2\mu_0} \right) v_n \mathrm{d}\sigma = 0, \tag{A6}$$

where W_k, W_g, W_i, and W_{m1} are the kinetic, gravitational, internal, and magnetic energies within the flux rope, respectively. Note that the volume integral of the last term in equation (A1) vanishes since $B_n = 0$ at the border of the flux rope. The surface integral in equation (A6) represents an energy flux going outside the flux rope. To avoid the complexity of calculating this surface integral, we presume that the energy variation outside the flux rope is dominated by magnetic energy, so the energy flux mentioned above approximately equals the variation of the magnetic energy outside the rope, denoted by W_{m2} hereafter. As a result, equation (A6) becomes

$$\frac{\mathrm{d}}{\mathrm{d}t}(W_k + W_g + W_i + W_m) = \frac{\mathrm{d}W_t}{\mathrm{d}t} = 0, \tag{A7}$$

$$\text{or} \quad W_k + W_g + W_i + W_m = W_t = \text{const}, \tag{A8}$$

where $W_m = W_{m1} + W_{m2}$ serves as the total magnetic energy of the system as a whole. We calculate W_k, W_g, W_i, and W_m at different times after catastrophe and found that equation (A7) or equation (A8) holds, with the relative errors being within a few percent. This implies that the presumption mentioned above is basically acceptable, and thus, equation (A8) may be used to quantitatively analyze the energy transformation during catastrophe.

Acknowledgments
This work was supported by the grants from NSFC (41774178, 41574165, 41421063, and 41274173), and the fundamental research funds for the central universities. The data and code scripts used in this paper can be found online at https://doi.org/10.6084/m9.figshare.5955616.

References

Chen, Y., Chen, X. H., & Hu, Y. Q. (2006). Catastrophe of coronal flux rope in unsheared and sheared bipolar magnetic fields. *The Astrophysical Journal*, *644*, 587.

Chen, Y., Hu, Y. Q., & Sun, S. J. (2007). Catastrophic eruption of magnetic flux rope in the corona and solar wind with and without magnetic reconnection. *The Astrophysical Journal*, *665*(2), 1421.

Chen, C., Wang, Y., Shen, C., Ye, P., Zhang, J., & Wang, S. (2011). Statistical study of coronal mass ejection source locations: 2. Role of active regions in CME production. *Journal of Geophysical Research*, *116*, A12108. https://doi.org/10.1029/2011JA016844

Ding, J. Y., & Hu, Y. Q. (2006). Coronal flux rope catastrophe in octapole magnetic fields. *Solar Physics*, *233*, 45–55.

Forbes, T. G. (2000). A review on the genesis of coronal mass ejections. *Journal of Geophysical Research*, *105*, 23,153–23,165.

Forbes, T. G., & Isenberg, P. A. (1991). A catastrophe mechanism for coronal mass ejections. *The Astrophysical Journal*, *373*, 294–307.

Forbes, T. G., & Priest, E. R. (1995). Photospheric magnetic field evolution and eruptive flares. *The Astrophysical Journal*, *446*, 377.

Golubitsky, M. (1978). An introduction to catastrophe theory and its application. *SIAM Review*, *20*, 352–387.

Guo, W. P., & Wu, S. T. (1998). A magnetohydrodynamic description of coronal helmet streamers containing a cavity. *The Astrophysical Journal*, *494*, 419–429.

Hu, Y. (1989). A multistep implicit scheme for time-dependent 2-dimensional magnetohydrodynamic flows. *Journal of Computational Physics*, *84*, 441–460.

Hu, Y. Q. (2001). Catastrophe of coronal magnetic flux ropes in partially open magnetic fields. *Solar Physics*, *200*, 115–126.

Hu, Y. Q., Li, G. Q., & Xing, X. Y. (2003). Equilibrium and catastrophe of coronal flux ropes in axisymmetrical magnetic field. *Journal of Geophysical Research*, *108*(A2), 1072. https://doi.org/10.1029/2002JA009419

Hu, Y. Q., & Wang, Z. (2005). Energy buildup of partly open bipolar field by photospheric shear motion. *The Astrophysical Journal*, *623*(1), 551.

Isenberg, P. A., Forbes, T. G., & Demoulin, P. (1993). Catastrophic evolution of a force-free flux rope: A model for eruptive flares. *The Astrophysical Journal*, *417*, 368.

Li, G.-Q., & Hu, Y.-Q. (2003). Magnetic energy of force-free fields with detached field lines. *Chinese Journal of Astronomy and Astrophysics*, *3*(6), 555.

Lin, J., Forbes, T. G., & Isenberg, P. A. (2001). Prominence eruptions and coronal mass ejections triggered by newly emerging flux. *Journal of Geophysical Research*, *106*, 25,053–25,074. https://doi.org/10.1029/2001JA000046

Lin, J., Soon, W., & Baliunas, S. L. (2003). Theories of solar eruptions: A review. *Nucleic Acids Research*, *47*, 53.

Low, B. C. (2001). Coronal mass ejections, magnetic flux ropes, and solar magnetism. *Journal of Geophysical Research*, *106*, 25,141–25,163. https://doi.org/10.1029/2000JA004015

Peng, Z., & Hu, Y.-q. (2005). Coronal mass ejections, magnetic flux ropes, and solar magnetism. *CAA*, *29*, 396.

Saunders, P. T. (1980). *An Introduction to Catastrophe Theory*. Cambridge: Cambridge University Press. https://doi.org/10.1017/CBO9781139171533

Subramanian, P., & Dere, K. P. (2001). Source regions of coronal mass ejections. *The Astrophysical Journal*, *561*, 372–395.

Sun, S. J., & Hu, Y. Q. (2005). Coronal flux rope catastrophe in the presence of solar wind. *Journal of Geophysical Research*, *110*, A05102. https://doi.org/10.1029/2004JA010905

Zhang, Q., Wang, Y., Hu, Y., & Liu, R. (2016). Downward catastrophe of solar magnetic flux ropes. *The Astrophysical Journal*, *825*, 109.
Zhang, Q., Wang, Y., Hu, Y., Liu, R., & Liu, J. (2017). Influence of photospheric magnetic conditions on the catastrophic behaviors of flux ropes in solar active regions. *The Astrophysical Journal*, *835*(2), 211.
Zhang, Y. Z., Hu, Y. Q., & Wang, J. X. (2005). Double catastrophe of coronal flux rope in quadrupolar magnetic field. *The Astrophysical Journal*, *626*, 1096–1101.
Zhou, G., Wang, J., & Cao, Z. (2003). Correlation between halo coronal mass ejections and solar surface activity. *Accident Analysis & Prevention*, *397*, 1057.